



# Measuring the Magnetic Field in Steel Using Flux Loops

**V.I. Klioukhine, R.P. Smith**

*FNAL, Batavia, USA*

**H. Gerwig, J.P. Grillet, A. Hervé**

*CERN, Geneva, Switzerland*

**Twelfth International Magnet Measurement Workshop**

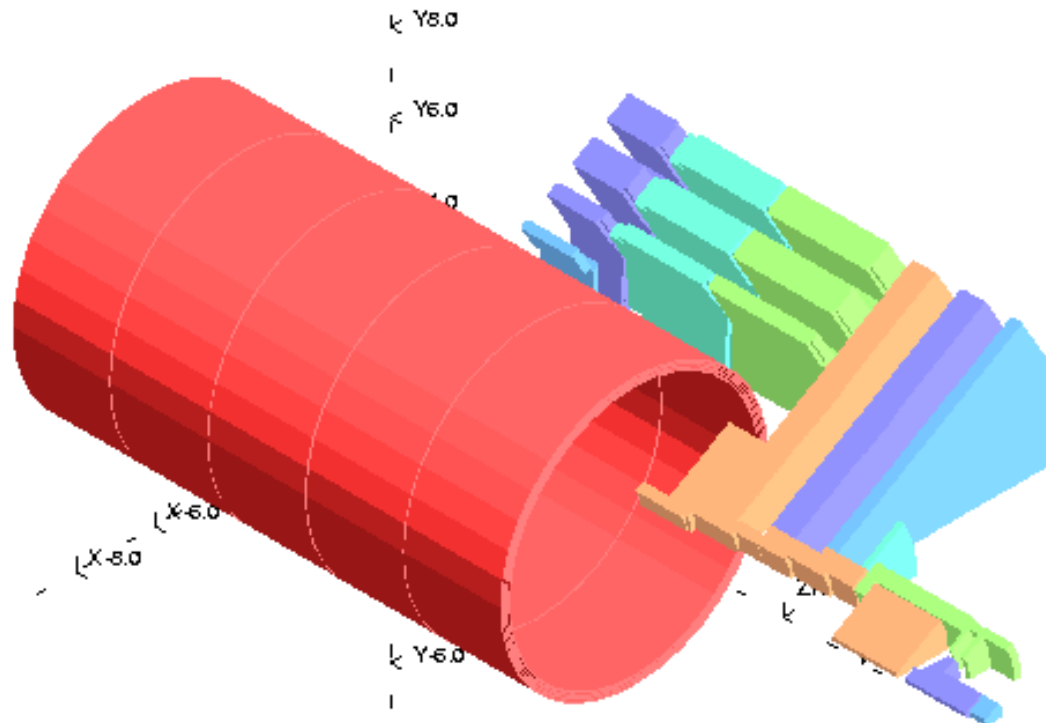
**ESRF, Grenoble, France - October 1-4, 2001**

# The CMS Magnetic System Model

The **Compact Muon Solenoid (CMS)** is a general-purpose proton-proton detector designed to operate at the **CERN Large Hadron Collider**. Its key feature is a **4 T superconducting solenoid** encased in a **12-sided three-layered steel “barrel”** with three-layered steel **“end-caps”**, comprised of steel plates up to **630 mm** thick, which return the flux of the solenoid and comprise the absorber plates of the **muon detection system**.

A **three-dimensional** magnetic field model of the **CMS** magnet has been prepared for utilization during the engineering phase of the magnet system, for early physics studies of the anticipated performance of the detector, as well as for track parameter reconstruction when detector operation begins.

# The CMS Magnetic System Model



**CMS Magnetic System Model Layout**

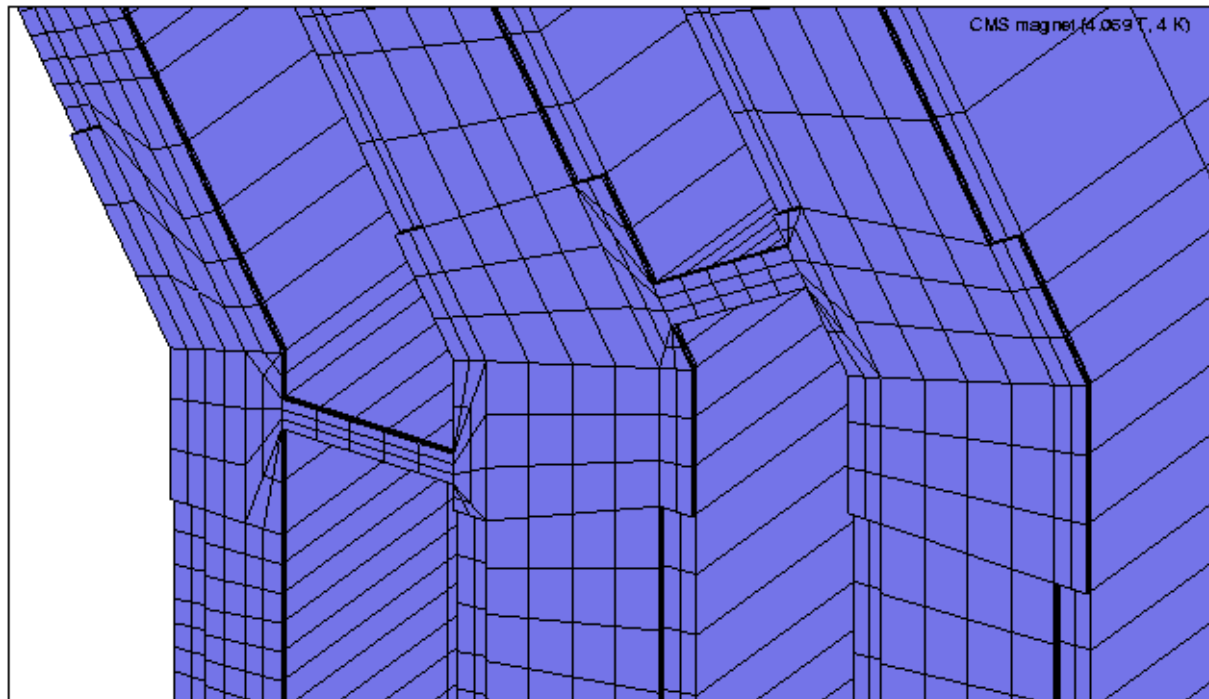
# The CMS Magnetic System Model

The **CMS magnetic system model** consists of the **superconducting solenoid coil** and includes **three** different geometries for the **14 m** diameter and **20 m** long **steel yoke** of the muon system. The latter obtained by reflection about  **$Z = 0$**  and symmetrizing an azimuthal segment subtending  **$30^\circ$**  to maximize the model precision.

The models of the yoke includes:

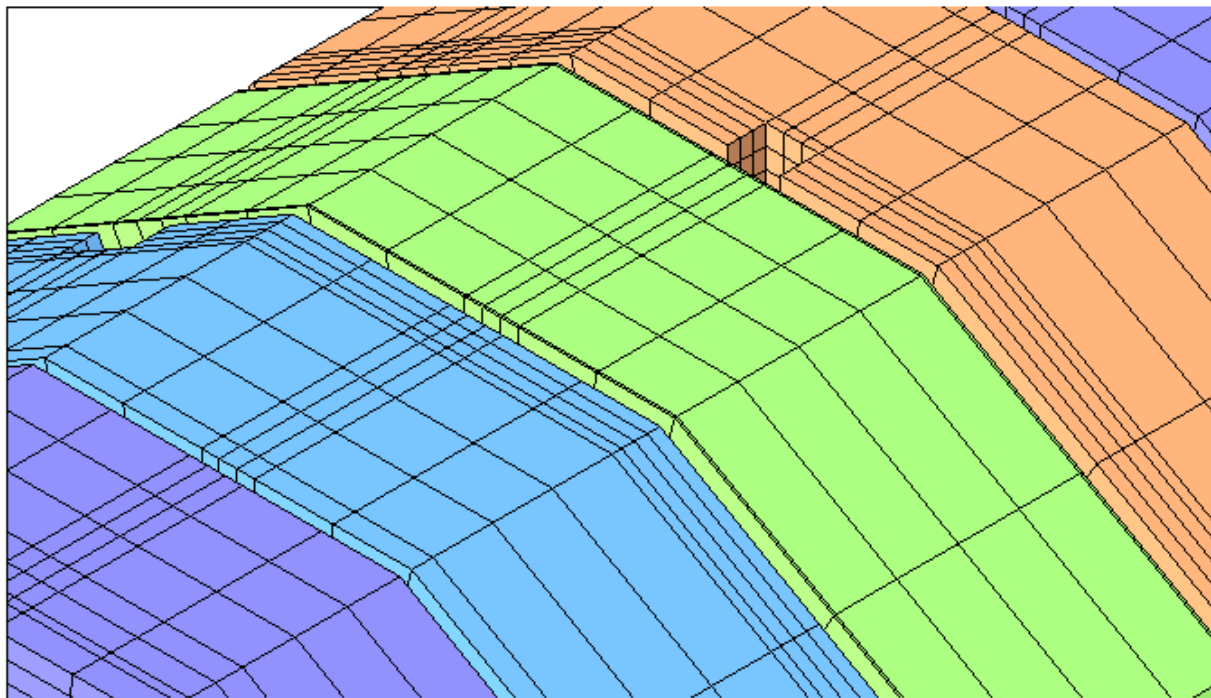
- the **barrel rings** with recessed outer plates, connecting brackets and two **chimneys**;
- the asymmetric **tail catcher**;
- the **nose disk**;
- **4 end-cap disks**;
- the hadronic **forward calorimeter ferromagnetic parts**.

# The CMS Magnetic System Model



**Brackets and the Recessed Plates View**

# The CMS Magnetic System Model



**Layout of Chimneys**

# The CMS Magnetic System Model

The **coil** is modeled as **20 cylinders of current** with dimensions corresponding to the positions of the superconducting cable in the winding layers when the coil is **at cryogenic temperatures**.

The radial thickness of each conducting cylinder is **20.63 mm**.

The cylinders form **4 coaxial layers of current** at internal radii **3174.93, 3240.06, 3305.19 and 3370.32 mm**, and they are grouped in **5 axially separated modules** spaced from one another by **45.86 mm**.

Each module has a length **2443.76 mm** and the overall axial length of the assembly is **12402.24 mm**.

# The CMS Magnetic System Model

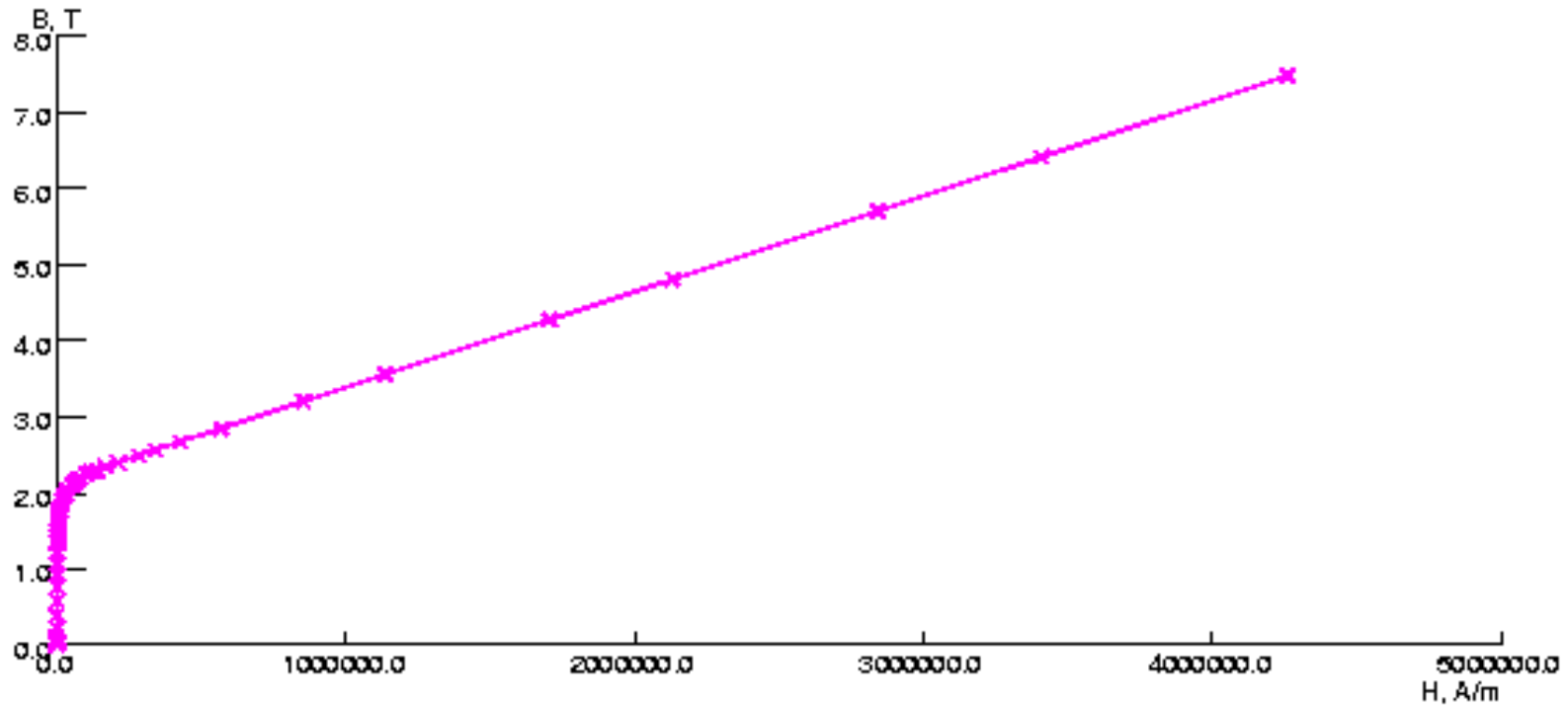
The **CMS** magnetic system model is performed using the **Vector Fields®** code **TOSCA** and the **Vector Fields OPERA-3d** post-processor.

**TOSCA** represents the field with **total** and **reduced scalar potentials** (accommodating accurately regions exterior to current sources as well regions containing current sources) and **the post-processor** calculates the magnetic field strength from **magnetization** and **current density sources**.

The models rely on use of “**averaged**” permeability values measured in many samples taken from the **muon steel plates**.



# The CMS Magnetic System Model



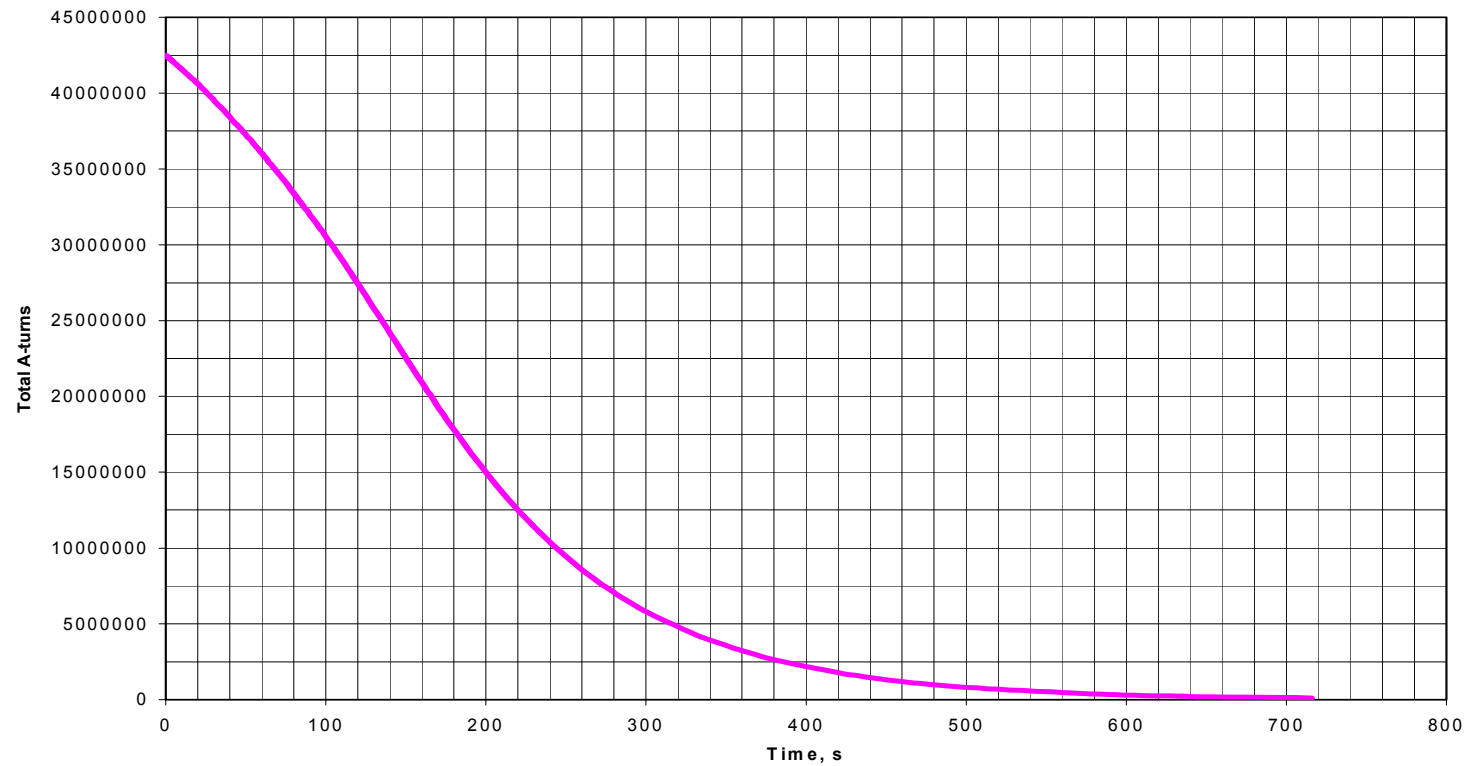
**One of the B-H Curves Used**

# Modeling the CMS Fast Discharge

It is desirable to provide a **direct measurement of the magnetic flux density** in select portions of the **muon steel** to help reduce the uncertainty in the measurement of the momenta of muons which penetrate the steel.

For this purpose, multi-turn **flux loops** have been installed around select segments of the **CMS** muon steel yoke plates to permit the measurement of changes in the magnetic flux density induced in the steel when the field in the solenoid is changed. The **rapid discharge** of the solenoid (approximately **300** seconds time constant) made possible by the protection system of the **superconducting solenoid** will induce significant **voltages** in the **flux loops**.

# Modeling the CMS Fast Discharge



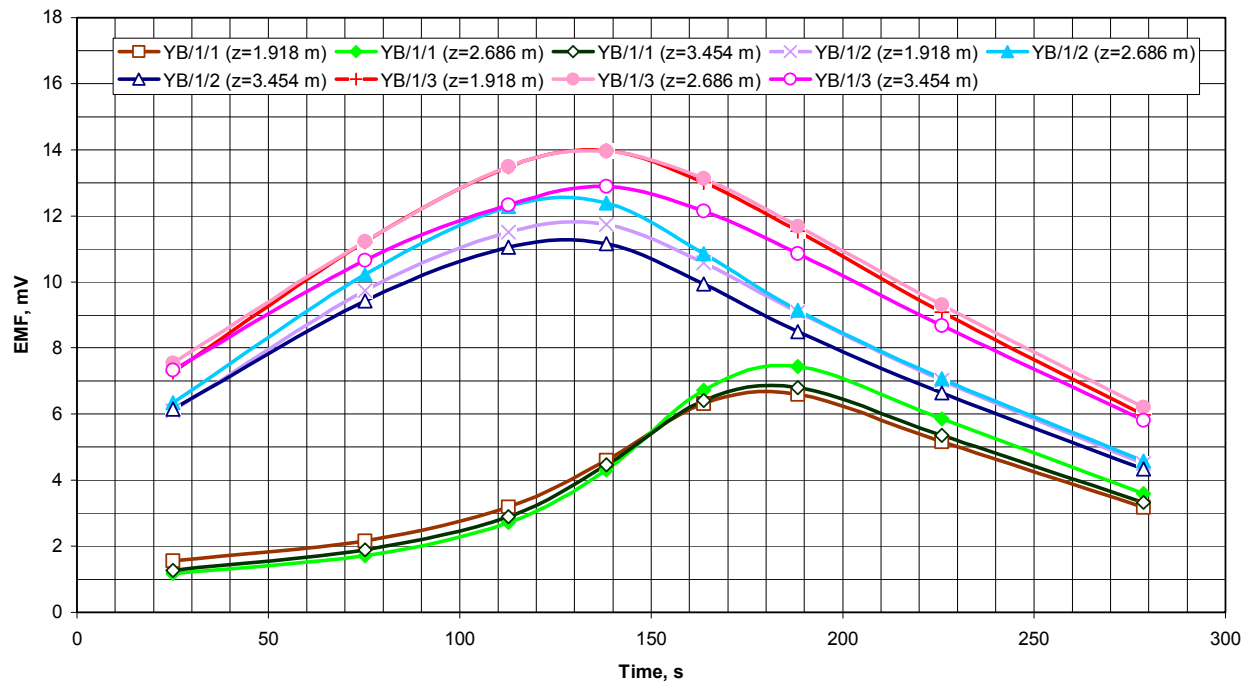
**CMS Coil Fast Discharge**

# Modeling the CMS Fast Discharge

At **9** discrete times (**0, 50, 100, 125, 151, 176, 200, 251, and 306** s) during the above discharge the fields were calculated in the detector, and in the plates of the barrel and endcap muon yoke steel the resulting **flux density** values were integrated over the areas enclosed by the **flux loops** at each time step.

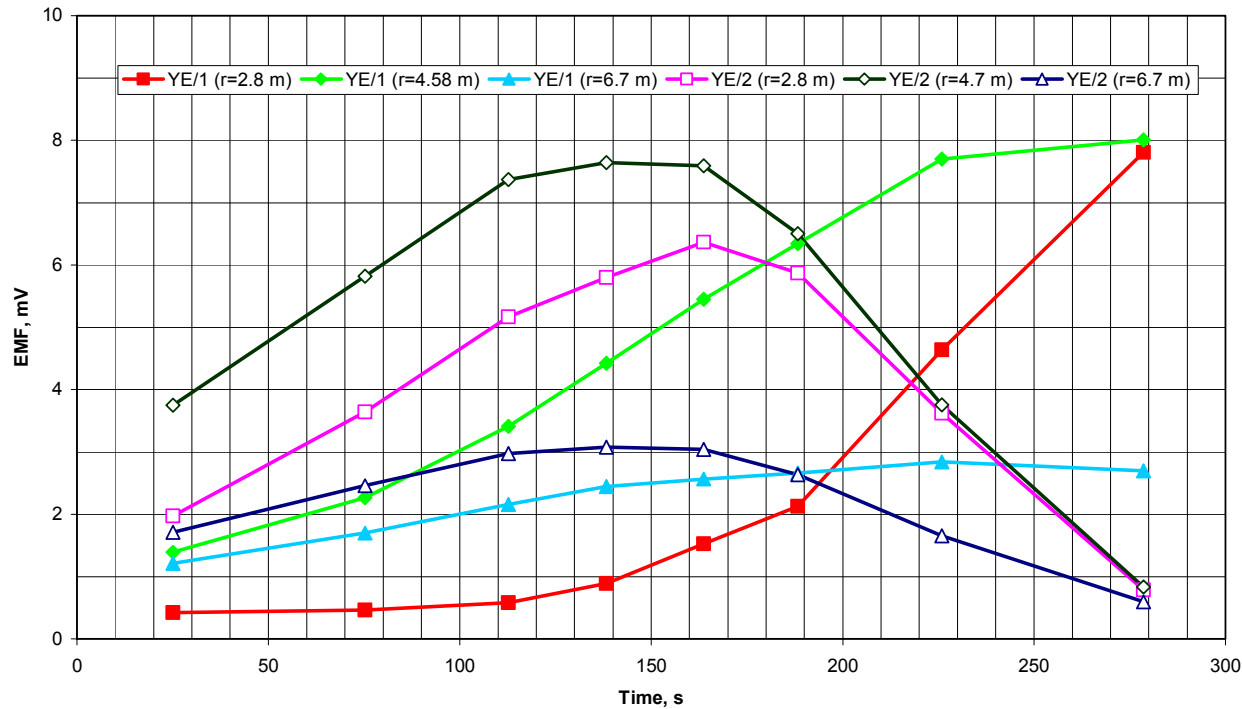
From the total flux  $\Phi$  enclosed by each loop the **average voltages**  $V=d\Phi/dt$  induced in the **loops** by the **flux changes** between the time intervals were calculated.

# Modeling the CMS Fast Discharge



## EMF per One-Turn Flux Loop in Barrel Plate Segments

# Modeling the CMS Fast Discharge



## EMF per One-Turn Flux Loop in End Cap Plate Segments

# Measuring Flux Changes in the CMS Steel

It is the goal of this study to determine if these flux coil **voltages** can be integrated over the **entire discharge** with sufficient accuracy to provide a measurement of the total **change of flux density** in the steel to a **few percent uncertainty**.

The technique of choice for the measurement of the voltages on the **flux coils** is the use of a **precision voltage sampling data acquisition system** with **fast ADC read out**, operating under the control of a **PC**. This technique avoids the need for high-stability integrators that must operate for long times.

# Experimental Approach

A **994**-turn model **flux coil** approximately **13.5 cm** in diameter was wound on a non-metallic coil former and connected to the selected sampling circuitry (**National Instrument DAQ Card 6012® PCMCIA module**) in **differential mode** to reject common-mode noise.

The **flux coil** was mounted between the **steel pole tips** of a laboratory standard **electromagnet** (**GMW® Model 3474**, energized with **Danphysik® Model 8530 power supply** equipped with **GPIB control interface**), and the magnet **charged** and **discharged** at a number of different rates under control by the same software used to sample the **voltage** on the model **flux coil**.



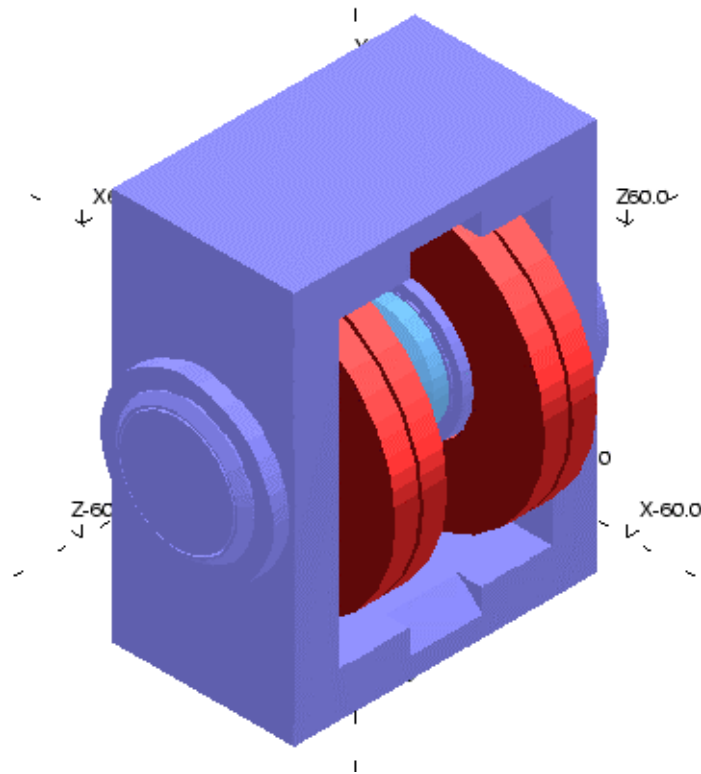
# Experimental Approach

In addition to studying the behavior of the “air core” flux coil, a steel disc was inserted in the coil to study the behavior of the coil when it encloses ferromagnetic material. An aluminum disc was also inserted in the flux coil to monitor eddy current effects.

A **TOSCA model** for the laboratory standard magnet was prepared to guide the interpretation of the data obtained from the **flux coil**.

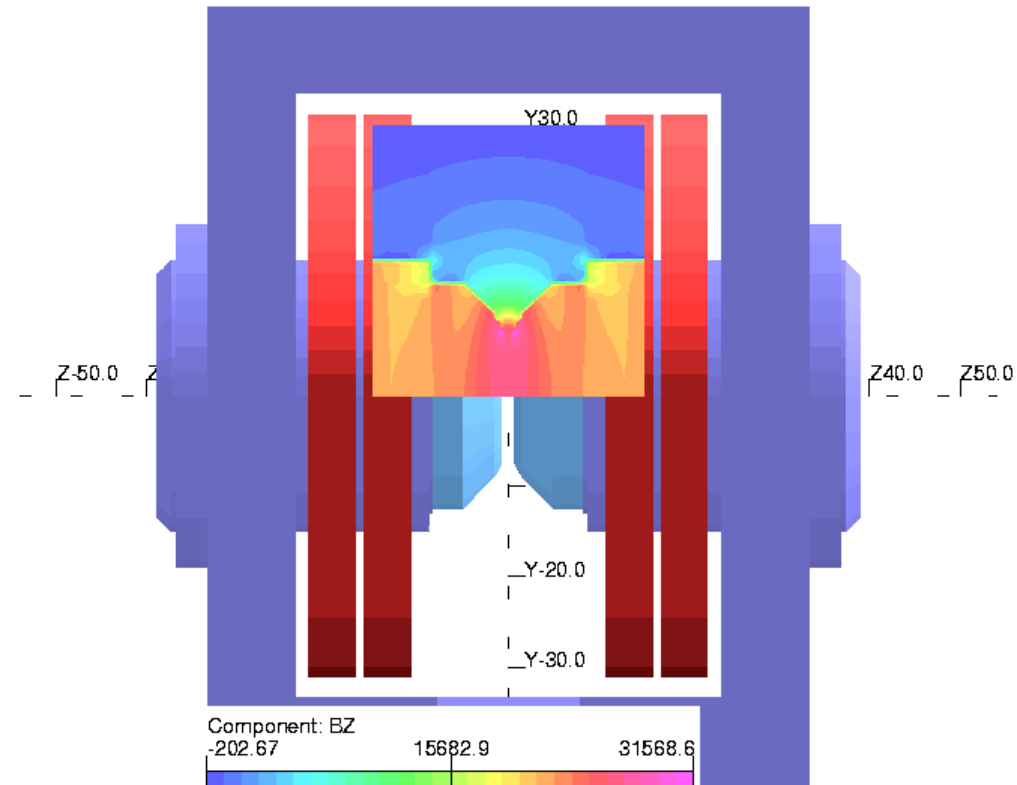
Values for the **B-H** data for the steel pole tips and yoke of the standard magnet were taken from those measured for the **CMS** yoke elements.

# Experimental Approach



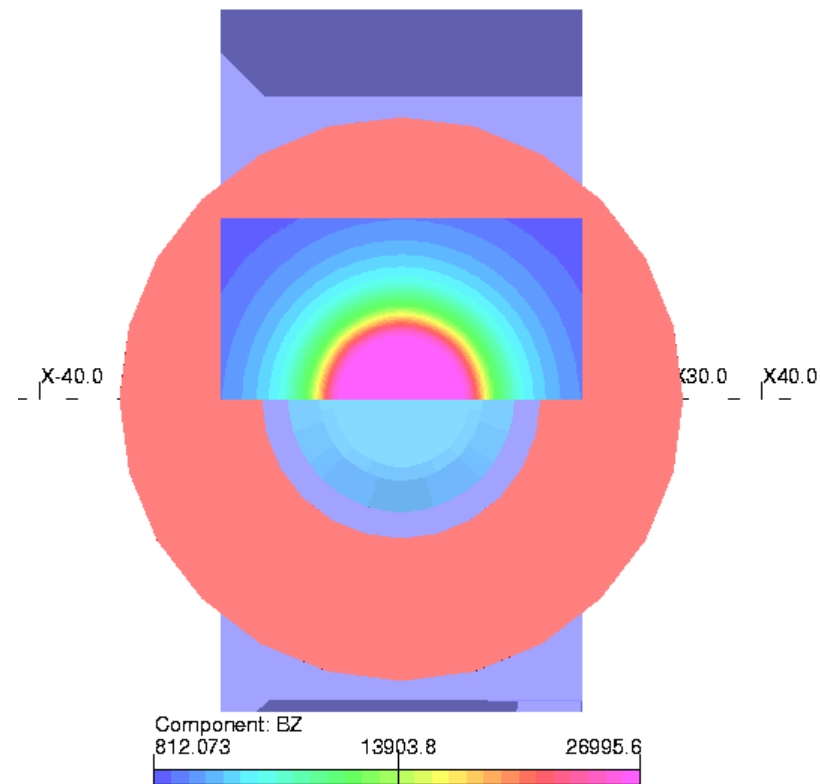
**TOSCA Model for Standard Magnet**

# Experimental Approach



**Axial Magnetic Induction in YZ-plane (Air Gap Case)**

# Experimental Approach



**Axial Magnetic Induction in Middle Plane of Air Gap**

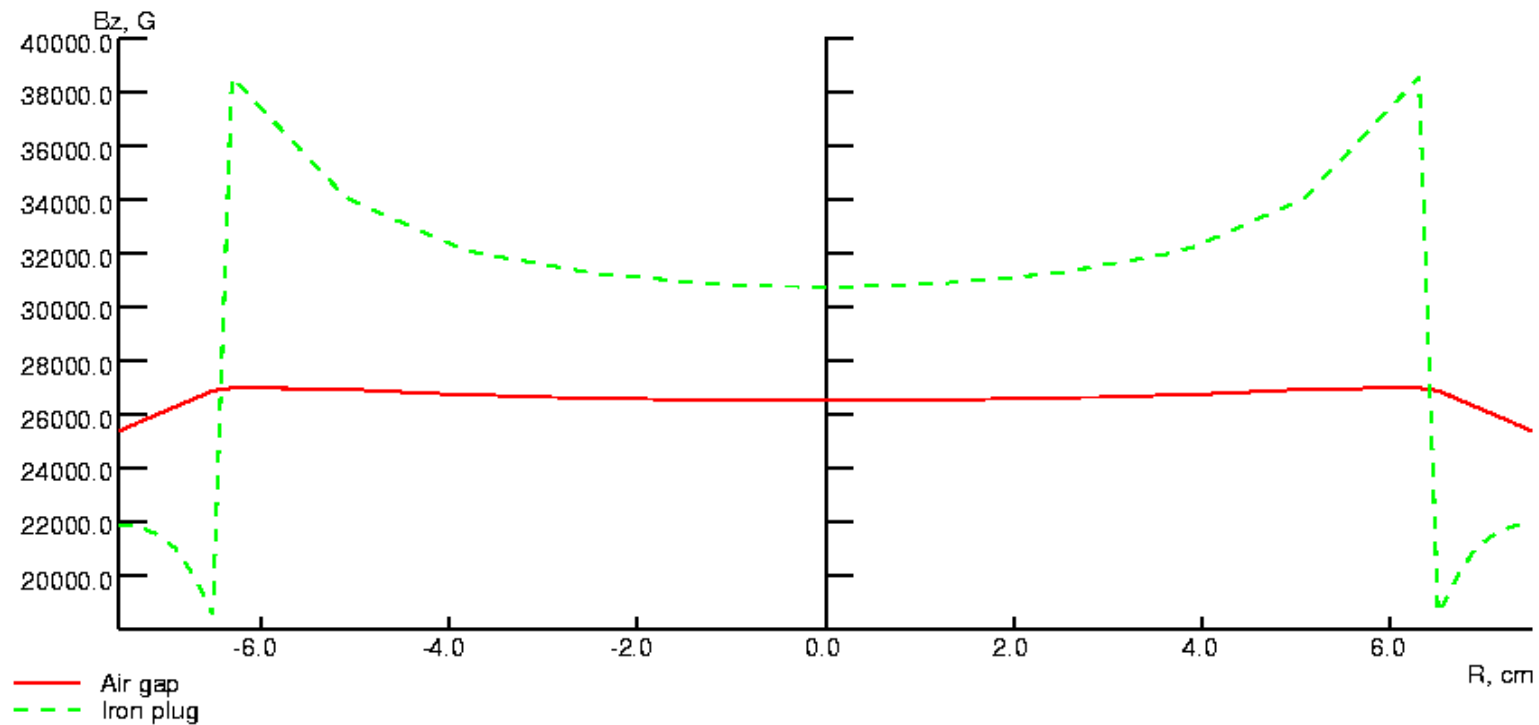
# Experimental Approach

The **TOSCA** model predicts closely the **flux density** in the **gap** (**2.65 T**) vs. that measured by **hall probes** (**2.63 T**) positioned on the surface of the pole tips when the magnet was energized **without** the **flux coil** in the **gap**.

When an iron **disc** was inserted in the **gap** the model predicts a field of **3.07 T** in the center of the **disc**.

For both the **air-gap** and **iron-filled gap**, the predicted field shape **rises** with **increasing radial distance** from the center of the pole tips.

# Experimental Approach



**Calculated Field in the Gap of the Standard Magnet**

# Data From the Model Coil

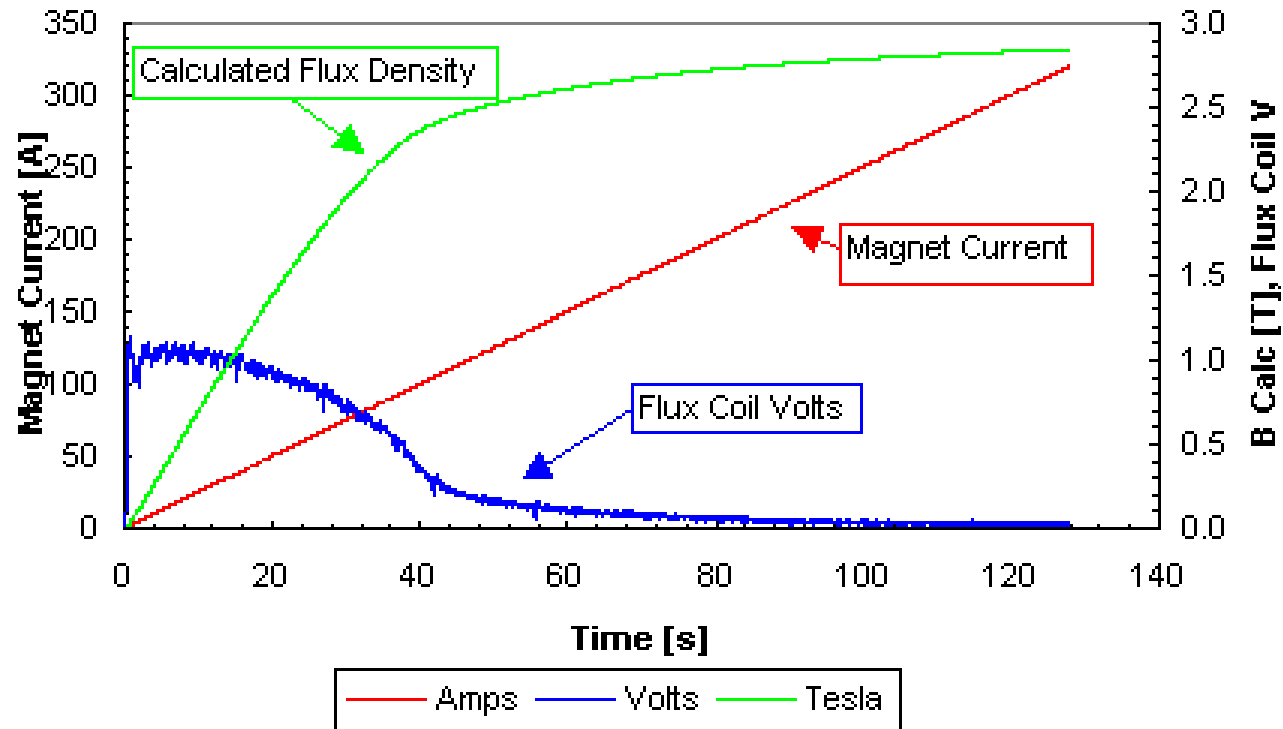
The **flux coil** was inserted in the standard magnet and the magnet **charged to full current** at a charge rate of **2.5 A/s**.

After a pause, **the current was decreased** at the same rate to **zero**. The **voltage** on the flux coil was **sampled** at **40 msec** intervals, and **integrated off-line** by simply multiplying the **average voltage** in each time interval by the **length** of the time interval.

The **measured flux change** from **charging** (**40.9 Webers**) and **discharging** (**40.0 Webers**) agree within **~2%**, provided added time (**~3 seconds**) is allowed at the end of the discharge cycle after the current has reached zero, for the pole tips of the magnet to **spontaneously demagnetize**.

# Data From the Model Coil

## Chargeup, No Iron

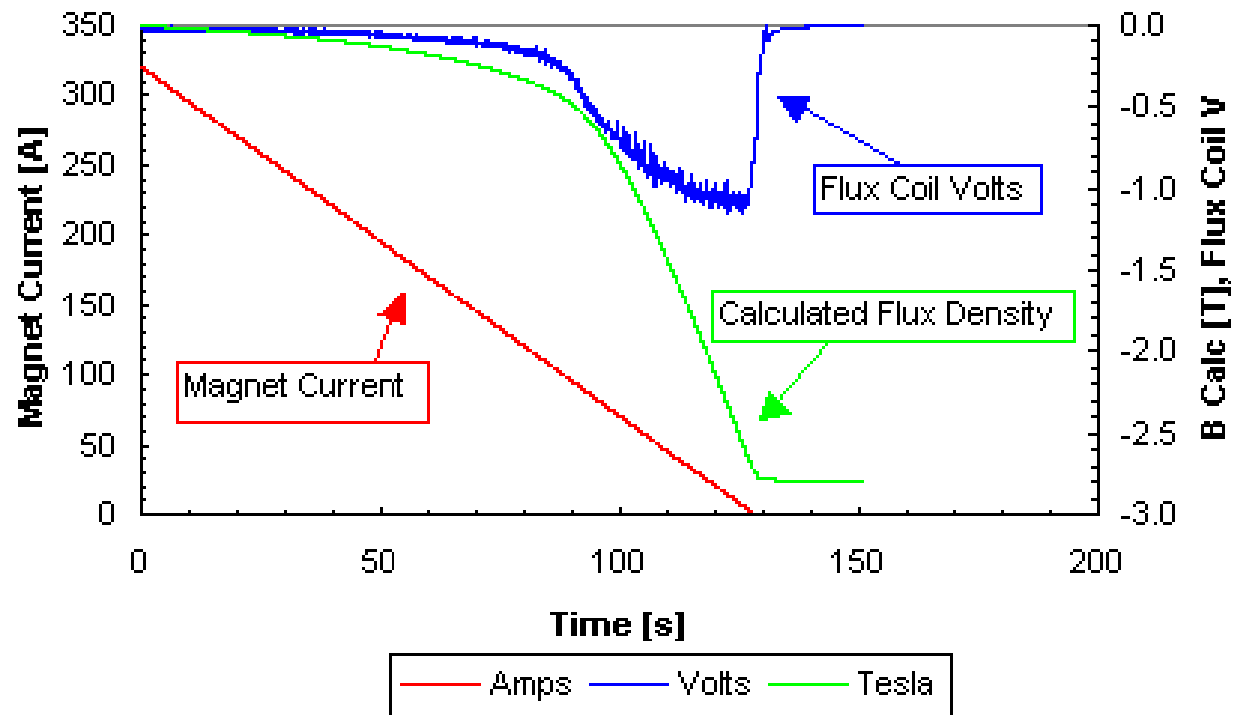


## Flux Coil in Air Gap, Chargeup



# Data From the Model Coil

## Discharge, No Iron



## Flux Coil in Air Gap, Discharge

# Data From the Model Coil

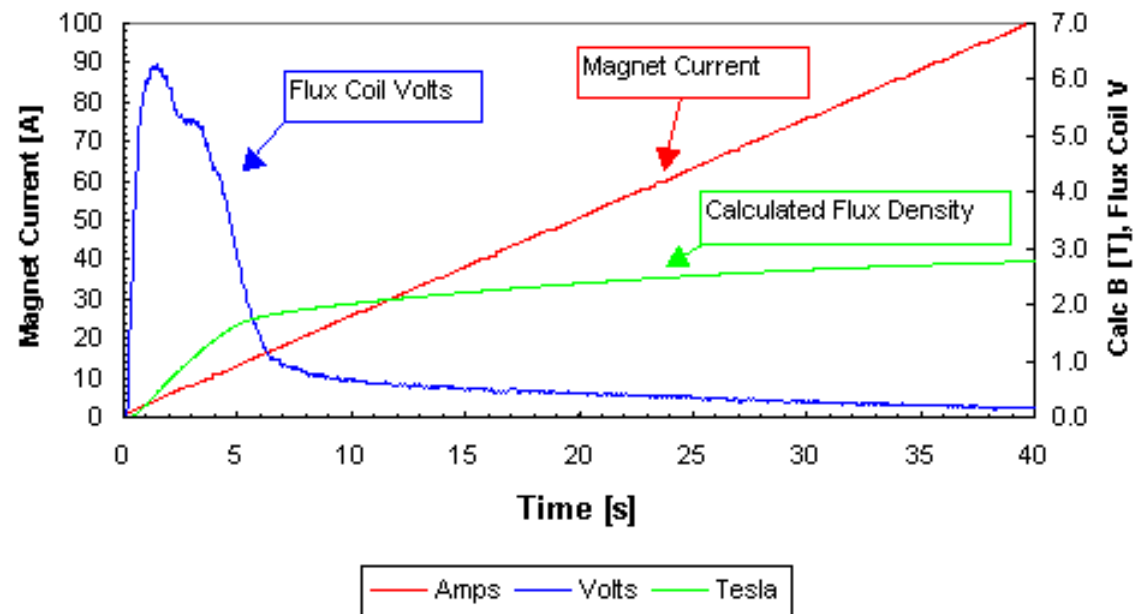
In the plots, the **flux** has been renormalized to **flux density** using the **area** of the **flux coil** and the **number of turns** in the coil.

The experiments were repeated after inserting a **high-carbon steel disc** in the **bore** of the **flux coil**.

The voltage on the **flux coil** during the early portion of the chargeup is large, reflecting the **rapid initial magnetization** of the **steel disc**.

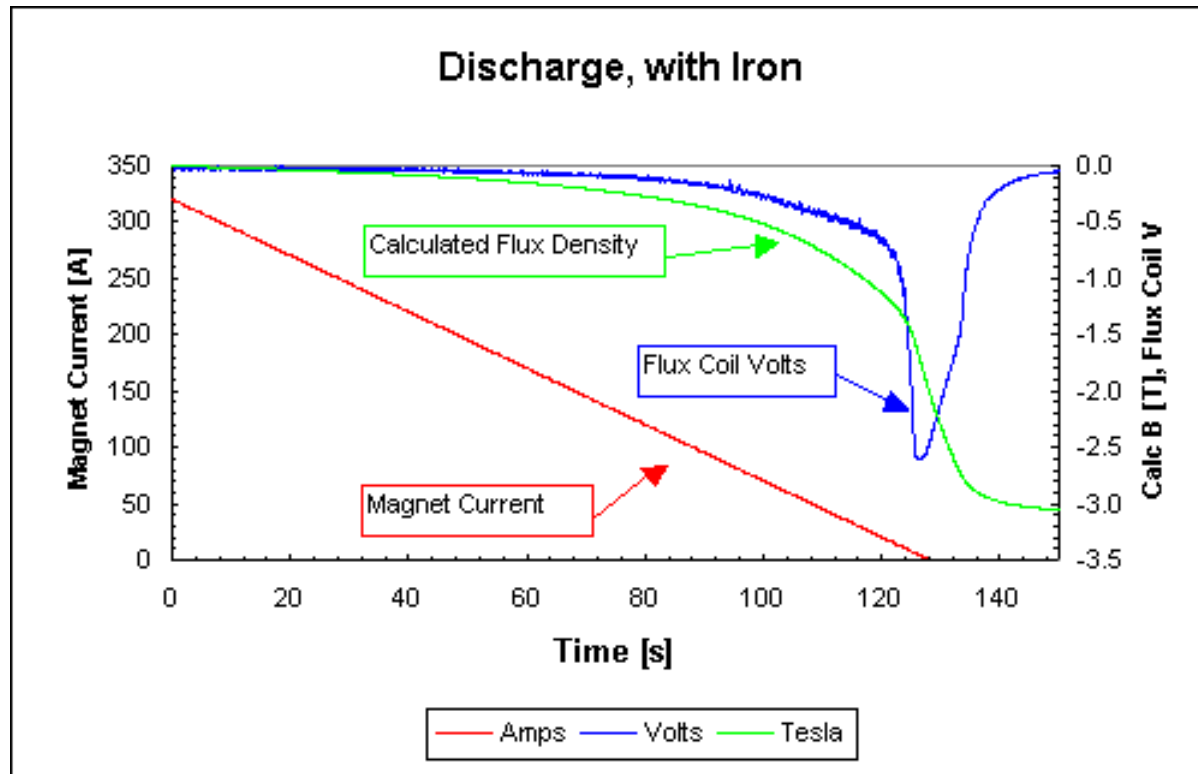
# Data From the Model Coil

Chargeup, with Iron



## Flux Coil With Iron, Detail from Early Portion of Chargeup

# Data From the Model Coil



## Flux Coil With Iron, Discharge

# Data From the Model Coil

The **measured flux change** during **chargeup** was **44.9 Webers**, and during **discharge** **44.6 Webers**. Note the full discharge of the system now requires **~15 seconds** additional time after the magnet current reaches zero, for the **spontaneous demagnetization** of the steel disc and the pole tips of the magnet.

Integrating the **TOSCA prediction** for the case with **steel** in the **flux coil** over the **area** of the **flux coil** yields a prediction in reasonable agreement with the **measured value**.

The **agreements** with **TOSCA** as well as the **equality of the flux changes** during **charging** and **discharging** indicate that the precision of the measurements is within **~2%**.

# Conclusions

- The experimental program described herein indicates that the increase of **flux density** in a **steel object** magnetized by an external source can be measured with **good precision** using a **fast sampling ADC** operating in **differential mode**.
- It is straightforward to **log the data** from a **flux coil** at **high speed** and **integrate the voltage off line** to obtain the total flux change in the coil.
- The observed remnant field effects in steel, of the quality and geometry studied, suggest that the demagnetizing fields in the CMS steel after discharge may be large enough to reduce the unmeasured flux of the remnant fields to low values.

# Future Plans

- **Ongoing laboratory work** will focus on studying the characteristics of such measurements using **steel samples** taken from the **yoke pieces** of the **CMS** magnet.
- Slower **charge** and **discharge rates** will be studied to verify that the somewhat longer **CMS** discharges will be accurately sampled, and to confirm that **eddy currents** are not significant. Studies made with an aluminum disc in the flux coil indicate that they are not.
- **Resistive discharges** of the **laboratory magnet** will be attempted to quantify the degree to which **voltage steps** of controlled **charging** and **discharging** are sources of error.